NASA TECHNICAL REPORT

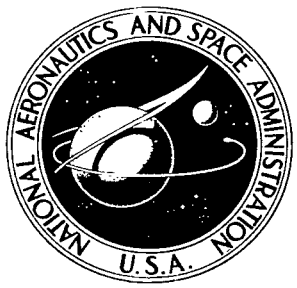

NASA TR R-290

NASA TR R-290

ELECTRON SPIN RESONANCE OF LITHIUM-DIFFUSED SILICON

by F. E. Geiger

Goddard Space Flight Center
Greenbelt, Md.

NATIONAL AERONAUTICS AND SPACE ADMINISTRATION • WASHINGTON, D. C. • AUGUST 1968

ELECTRON SPIN RESONANCE OF LITHIUM-DIFFUSED SILICON

By F. E. Geiger

Goddard Space Flight Center
Greenbelt, Md.

NATIONAL AERONAUTICS AND SPACE ADMINISTRATION

For sale by the Clearinghouse for Federal Scientific and Technical Information
Springfield, Virginia 22151 – CFSTI price $3.00

ABSTRACT

Electron paramagnetic resonance was studied in floating-zone, lithium-diffused silicon. The resonances observed were identified as the result of (Li-O) complexes. The g-factor for the (Li-O) complex with the magnetic field H_0 in the $\langle 100 \rangle$ direction was found to be in good agreement with the calculated value obtained from the principal g-factors determined by Feher for crucible-grown silicon. Instrument sensitivity allowed the recording of (Li-O) and phosphorus donor hyperfine structure, thus permitting the (Li-O) concentration to be determined and the oxygen concentration in floating-zone silicon to be estimated. Irradiation of floating-zone, lithium-diffused silicon emptied the phosphorus donor levels and about 54 percent of the (Li-O) levels into deep traps; however, no new centers were found, although an unidentified structure was observed at approximately g = 2.006. The lithium-diffused sample of 0.16 ohm-cm resistivity gave a narrow (0.9 oersted), stress-sensitive resonance line. The resonance split into a doublet in the $\langle 100 \rangle$ direction. The observed anisotropy and splitting of the resonance were fitted to a spheroidal g-tensor of $\langle 100 \rangle$ axial symmetry with principal g-values $g_{\parallel} = 1.99969 \pm 0.00015$ and $g_{\perp} = 1.99908 \pm 0.00015$. The resonance was attributed to lithium donor electrons in a $\{E + T_1\}$ ground state and donor wave functions arising from single conduction electron valleys.

CONTENTS

ELECTRON SPIN RESONANCE OF LITHIUM-DIFFUSED SILICON

by
F. E. Geiger
Goddard Space Flight Center

INTRODUCTION TO PROBLEM

The electron spin resonance signal of lithium-doped or diffused silicon was first observed by Honig and Kip (Reference 1) in a sample of silicon containing 7×10^{16} lithium atoms per cm^3.* The observed resonance absorption line had a full width at half maximum of 1.5 oersted and apparently an isotropic g-factor of 1.999. The resonance showed r.f. power saturation characteristics of inhomogeneously broadened resonance lines. The line shape was found to be approximately gaussian. The four hyperfine components because of the interaction of the electron and the Li nucleus were estimated to have a separation between components of about 0.1 oersted. The estimated hyperfine interaction should have produced a flattening of the observed resonance line, but none was observed. Feher (Reference 2) observed the lithium donor resonance in a silicon sample containing 3×10^{16} lithium atoms per cm^3. His observation was at considerable variance with the results reported by Honig and Kip (Reference 1). The resonance line was again inhomogeneously broadened, but found to have had an anisotropic g-value and a line width of 2.3 oersted. The g-tensor was found to be axially symmetric with the axis of symmetry in the $\langle 111 \rangle$ direction. Significantly enough, the resonance line was found in the dispersion mode. Feher was able, by means of the ENDOR technique (Reference 3) to find the hyperfine spectrum of the interaction of the donor electron with the Li^7 nucleus. Feher finds a hyperfine interaction constant for Li^7 of 0.845 MHz, corresponding to a separation of the Li hyperfine lines of about 0.3 oersted. Feher also investigated floating-zone silicon which had been doped to the same concentration of lithium atoms as the above-mentioned crucible-grown silicon. No resonance signal was observed, from which it was concluded that oxygen was necessary for the formation of a paramagnetic defect with lithium. It is interesting to note here that Feher does not comment on the significant difference between his results and those of Honig and Kip.

Considerable light was thrown on the lithium donor situation in silicon by the work of Aggarwal et al. (Reference 4). Aggarwal et al. investigated the excitation spectra of lithium donors in silicon and were able to observe both the spectrum caused by lithium itself and lithium-oxygen complexes. Identification of the two spectra was achieved by comparison with the excitation spectra of group-V donors in silicon under zero and uniaxial stress. Further, on the basis of their stress experiments,

*Determined by Hall effect measurements.

Aggarwal et al. were able to determine the symmetry of the ground state of both the lithium donors as well as the lithium-oxygen complexes in silicon.

In the theory of shallow donors (group-V atoms in silicon) developed by Kohn and Luttinger (References 5 and 6), the donor electron of effective mass m^* moves in the coulomb potential of the donor atom in a medium of static dielectric constant κ. Since the conduction band minimum of silicon does not occur at $k = 0$, but at points $\langle k_0, 0, 0\rangle$ inside the Brioullin zone, there will be six equivalent conduction band minima. Thus in the effective mass approximation, there will be six equivalent solutions associated with the six equivalent conduction band minima. When corrections are made to the effective mass theory, the sixfold degeneracy can be partially lifted. The remaining degeneracy may be found from the character table of the tetrathedral point group T_d, the symmetry of the donor atom in the silicon lattice. Comparison of the characters of the irreducible representations of T_d and those of the representation $\{1s\}$ of the basis functions of the ground state found from the effective mass theory, show that $\{1s\}$ breaks into

$$\{1s\} = A_1 + E + T_1 . \tag{1}$$

The dimensionality of A_1, E, and T_1 is respectively one, two, and three. Only the singlet A_1 gives a finite probability for the electron to be at the donor site. Since in this region the effective mass approximation is expected to break down, we expect the level corresponding to the singlet state A_1 to be split off from the approximately degenerate doublet E and triplet T_1. The symmetry arguments presented here do not determine to which representation the lowest level belongs. However, singlet state A_1 is the only state which gives a nonvanishing probability for the electron to be at the donor atom. Consequently, one would expect a strong hyperfine interaction for a donor electron in the singlet state but none for the doublet or triplet. Feher's (Reference 2) results prove conclusively that in silicon the donor electron ground state is a singlet for phosphorous, arsenic, and antimony donor atoms. The implications of the above analysis are quite clear. A degenerate ground state belonging to a multidimensional representation of T_d will make observation of electron spin resonance of the donor electron difficult if not impossible. Partial lifting of the degeneracies of the ground state by internal and external strains will probably result in the observation of resonance lines of varying width, intensity, and g-values. The apparent disparities in the results of Feher (Reference 2), Honig and Kip (Reference 1), and Watkins (Reference 7) are strong indications that lithium donors have a degenerate ground state.

Aggarwal et al. (Reference 4) found their excitation spectra of crucible-grown and floating-zone silicon to be consistent with the following picture. The (Li-O) complex found in crucible-grown silicon ($N_D = 6 \times 10^{15}$ lithium atoms per cm^3) has tetrathedral site symmetry (point group T_d), the lowest ground state is the singlet A_1 of the group-V-like ground state, and the excitation spectrum only occurs in the crucible-grown sample. The excitation spectrum of floating-zone silicon ($N_D = 1 \times 10^{15}$ lithium atoms per cm^3) is consistent with tetrahedral symmetry of the isolated lithium, and inverted group-V ground state; i.e., the singlet A_1 is now above the degenerate double E and triplet T_1. Again the spectrum for floating-zone silicon is not observed in crucible-grown silicon. Watkins (Reference 7) using a sample of Aggarwal's lithium-diffused floating-zone silicon, observed

the electron spin resonance of the lithium donor electron. At 4.2°K, the resonance was 20 oersteds wide and anisotropic with an approximate g-value of 2.006. Small, uniaxial stresses cause the broad line to disappear and to reemerge at a sharp line (≲1 oersted) with a g-value of 1.998—2.001. Although Watkins' results are in agreement with Aggarwal's conclusions, Honig and Kip's seem not. Our own preliminary experiences with lithium-diffused floating-zone silicon were so at variance with any of the aforementioned results that it seemed worthwhile to reexamine the electron spin resonance spectrum without the application of uniaxial stresses. Generally speaking, however, any rational explanations of observed ESR spectra of lithium-diffused silicon are probably doomed without uniaxial stress experiments.

EXPERIMENTAL DETAILS

Experimental Equipment

The electron spin resonance spectrometer used in these experiments was a balanced bridge type with homodyne detection. At the beginning of the experiments, a balanced bridge type with superheterodyne detection was used, but it presented so many problems for the particular kind of experiments we were doing that it was abandoned in favor of a homodyne bridge. The basic spectrometer set up was a Varian Associates V-4502-15 system with a superheterodyne attachment. The signal klystron is stabilized by frequency modulation of the microwave C.W. and locks to the sample cavity. The advantage of this method is the detection of a pure absorption mode (once the bridge is properly balanced) without admixture of the dispersion mode. The difficulty with such a system is twofold. For observation of the dispersion mode, an external reference cavity must be used, which makes bridge balance difficult. A more serious objection may be the effect of frequency modulation on the observation of inhomogeneously broadened lines with long relaxation times.* Frequency modulation, in effect, causes the individual spin packets to be traversed many times causing partial or total destruction of magnetization and, in some cases, complete saturation of the resonance line. This phenomenon is discussed in detail by Feher (Reference 2).

Actual observation of inhomogeneously broadened lines (such as phosphorus donor electrons in silicon, as well as A-centers and lithium-oxygen complexes in silicon) seemed to show that this effect was not very significant, although no detailed experiments were done to investigate the effect of frequency modulation. In order to avoid the cumbersome adjustment procedure of the superhet bridge, we switched to a simple homodyne bridge (again using the basic Varian Associates V-4502-15 system) but replaced the microwave detector (1N23F diode) with a selected L4154 Philco† backward diode.‡ Experiments showed that it was possible to use the diode with a magnetic field modulation frequency as low as 400 Hz and still get a signal-to-noise voltage ratio which was twice that obtained under the same conditions with the superheterodyne bridge. All measurements reported here were made with this homodyne bridge. The crystal bias was obtained from a slide-screw

*We are much indebted to G. D. Watkins of the General Electric Research Laboratory for calling this difficulty to our attention.
†Philco, Lansdale Division, Lansdale, Pennsylvania.
‡We are greatly indebted to Prof. R. H. Sands for this suggestion.

tuner in the reference arm of the bridge, and adjusted for a crystal current of 100 microamps. The rectangular cavity operated in the TE_{102} mode and was coupled to the waveguide with a combination coupling hole (diameter 5.0 mm) and capacitive coupling screw in a diaphragm 0.020 inch thick. A silver gasket between diaphragm and cavity flange insured good contact. The cavity was operated at critical match at liquid helium temperature. The rectangular cavity itself was made from a standard piece of X-band waveguide.

The magnetic field modulation frequency was in all cases 400 Hz. The modulation coils were of the usual Helmholtz configuration, 9.6 inch O.D. and separated by the gap of the 12-inch magnet, which was 4.5 inches. Each coil had 70 turns of AWG No. 22 wire, and a measured resistance of 2.85 ohms. The Helmholtz coils were fed by a McIntosh MC75 power amplifier. This combination produced a maximum magnetic sweep field amplitude of 10 oersteds at the sample mounted in the TE_{102} cavity at room temperature and at a modulation frequency of 400 Hz. All measurements were made with a modulation amplitude (at the sample) of about 0.1 oersted at liquid helium temperature.

The cryogenic equipment consisted of a conventional double glass dewar system. The temperature of the system was monitored with a 1/4-watt, 100-ohm carbon resistor. Resistance measurements were made with a Leeds & Northrup No. 4735 wheatstone bridge and No. 9834 null detector. The bridge was operated at a reduced voltage of about 20 mv. Liquid helium filled the waveguide assembly and cavity. Bubbling of helium in the cavity did not seem to present a serious problem. Experiments showed that any gain made by filling the cavity with styrofoam was offset by a reduction of the cavity Q by approximately a factor of two. A more serious problem was the effect of the dropping liquid helium level in the waveguide assembly. Dispersion measurements depend on a fairly accurate adjustment of the phase balance of the bridge. Once an adjustment had been made, it could only be maintained for about 20 minutes or half an hour, before the shifting liquid helium level required a complete rebalance of the bridge. The effect of the shifting helium level appeared to be much worse in the superheterodyne configuration of the bridge.

Magnetic field were measured with a Magnion Model G-502 nuclear magnetic resonance gaussmeter. The center of the photon sample in the gaussmeter probe was 1-5/32 inch from the center of the magnet pole piece. The magnetic field at the proton probe was 0.025 oersted higher than at the center of the pole pieces. Unfortunately, there was considerable interference between the 400-Hz electron spin resonance magnetic field modulation and the 60-Hz modulation of the proton probe. The circuits of the magnetometer were consequently modified to work at a 400-Hz modulation frequency and to take advantage of the electron spin resonance sweep field. Since it was possible to use ESR sweep fields of only 0.10 oersted amplitude, accurate field determinations could be made while the main field was being swept linearly and spin resonance lines were recorded. The considerably higher modulation frequency required a proton sample of shorter spin lattice relaxation time, and a new proton probe was made by adding sufficient Mn^{++} ions to distilled water to produce an acceptable proton resonance pattern. The linewidth of the photon resonance was about 0.3 oersted. Using a 400-Hz modulation frequency and the proton probe described above, it was possible to determine the magnetic field to within ±0.05 oersted.

Microwave frequency determinations were made with a Hewlett-Packard 0—20 MHz 5243L counter, with a 50—500 MHz frequency converter, Model 5253B, a Model 540B transfer oscillator, and a Dymec Model DY-5796 transfer oscillator synchronizer. This combination of units proved most convenient. The proton resonance frequencies were counted directly with the 5243L, whereas the transfer oscillator frequency (approximately 207 MHz) was counted by switching to the 5253B converter plug-in. The transfer oscillator synchronizer locks the transfer oscillator to the microwave signal frequency and maintains zero beat frequency between a multiple of the transfer oscillator frequency and the microwave signal. In other words, the synchronizer automatically tracks signal and transfer oscillator drifts.

The short-term frequency stability of the klystron (locked to the sample cavity or the reference cavity) was about 2 parts in 10^7 over a 3-minute period. The "absolute" accuracy of the frequency counter was determined by beating the standard frequency output of the counter against the 10-MHz frequency of Bureau of Standards station WWV in a Signal Corps R-390/URR Collins Radio Co. superheterodyne receiver. The 10-MHz timebase frequency was found to be within 7 cycles of the WWV standard; i.e. the short-term frequency drift of the klystron is less than the absolute frequency error of the 5243L counter. Microwave power requirements for the frequency counting setup were approximately 1 mw. Power was coupled directly from the klystron into the transfer oscillator by means of a 20-db cross-coupler; this could only be done after a considerable modification of the Varian V-4500-41A microwave bridge.

The microwave bridge adjustment is, on the whole, conventional. The power incident on the sample is fixed by two attenuators—one in the signal generator arm, the other an adjustable ferrite isolator in the sample cavity arm of the bridge.* The advantages of the adjustable isolator are to some extent offset by the large phase shifts it introduces. Calibration of the isolator phase shift as a function of attenuation proved impractical and nonreproducible. It therefore became necessary to first balance the bridge with the adjustable isolator set for the desired attenuation, (which is tricky if the attenuation is on the order of 20 db), then provide the proper bias on the detector crystal with the slide screw tuner in the reference arm.* The dispersion mode is detected by introducing a 90-degree phase shift by a phase shifter in the sample arm. The accuracy of adjustment of the bridge was checked by means of a small piece of ruby crystal, (Al_2O_3 plus 0.05 percent of Cr^{3+} by weight),† which also served as standard for relative comparisons of cavity Q's.

The bridge was usually operated at a power level of 36.5 db below klystron output, (230 mw at 9.3 GHz), or with actual power incident on the sample cavity 39.5 db below klystron power because of the magic "T". Power variations of more than 6 to 8 db above or below the 39.5-db value made it difficult to lock the AFC system to the reference cavity, severely limiting saturation measurements. No such difficulties were encountered when operating the bridge in the absorption mode with the klystron locked to the sample cavity. No experiments were made to determine the reason for the AFC lock-on difficulties in the dispersion mode.

*See R. C. Rempel and H. E. Weaver, *R. Sci. Inst.* 30, 137, 1959 for a discussion of the bridge and the adjustable ferrite isolator.
†The crystal was cut from a piece of ruby laser rod obtained from the Union Carbide Corp., Linde Div. Union, N. J. Rod diameter 0.125 inch, sample length for use in spectrometer, 3 mm. Rod axis parallel to c-axis of crystal.

The audio frequency circuits were conventional. The resonance signal was phase-detected by a Princeton Applied Research lock-in amplifier, Model JB-5, and recorded on a Leeds & Northrup Speedomax Azar recorder. The chart speed of the recorder was in all cases 60 inches/hr. The lock-in amplifier was usually operated with a time constant of 1 sec to 3 sec, and the magnetic field was swept linearly at a rate of 250 oersted in 50 minutes.

Silicon samples were cut from ingots and oriented optically (References 8 and 9) to better than ±2 degrees. The sample was cut with a No. 100 grit diamond saw to the dimensions of 9 mm × 20 mm × 0.5 mm and etched to remove paramagnetic centers created by the cutting operation (References 2 and 10). The sample orientation was chosen to allow orientation of the magnetic field in the {110} plane of the crystal (Reference 2): the 9 × 0.5 mm and the 20 × 0.5 mm face in the ⟨110⟩ direction, and the 20 × 9 mm face in the ⟨100⟩ direction. The sample was mounted on the narrow side wall (0.4 inch × 1.70 inch) of the TE_{102} cavity. Samples were fastened to the cavity walls with Duco cement when stresses were of no importance; in cases where the resonance was stress-sensitive, the sample was mounted on a special polystyrene holder which gripped one side of the sample but left the rest of the sample completely free. The holder itself was then glued to the cavity. This type of holder proved suprisingly successful from the point of view of noise created by vibrations of the relatively free sample, but produced a relatively large frequency shift which made the bridge balance difficult. The method of holding the sample in the cavity which was finally used consisted simply of wedging the sample between the cavity wall and a small piece of Styrofoam. This type of mounting gave good results with respect to freedom from electrical noise and external stresses. On the whole it seems difficult to design a sample mount which leaves the sample completely unstressed.

The lithium-diffused samples were prepared by spreading a suspension consisting of a mixture of lithium powder, mineral oil, and Al_2O_3* of more or less arbitrary proportions on the sample and diffusing it at a temperature of 485°C in an argon atmosphere for 1 hour. This procedure resulted in a very low resistivity silicon sample (on the order of 0.01 ohm-cm). To bring the resistivity to the required value of 0.2 ohm-cm, the sample was cleaned and then baked for 2 hours at 485°C. These figures are correct for floating zone, 400 ohm-cm, phosphorus-doped silicon and may be different for different dopant concentrations.†

Experimental Procedure

The primary purpose of this investigation was to find the structure of the lithium defects in silicon, and the structure of possible defects produced by electron irradiation and the presence of oxygen. The simplest form of the spin Hamiltonian $\mathcal{H}$,

$$\mathcal{H} = \beta S \cdot g \cdot H_0 , \qquad (1)$$

*Particle size 1 micron, made by Linde.

†The silicon diffusions and all the considerable work involving working out and investigating satisfactory diffusion procedures were done by Mr. W. Wauppus. The above techniques gave reproducible results and samples without surface damage. Resistivity measurements were made with a four-point probe made by A. & M. Fell Ltd., London, England. The all important information on the addition of Al_2O_3 powder to the lithium suspension came from Mr. E. Irwin, Westinghouse Corp., Baltimore, Md.

with an effective spin of 1/2, and the g-value a tensor quantity, will account for the anistropy and splitting of the observed spectrum (Reference 11). The main axes of the g-tensor will have the symmetry of the defect. If the defect has tetrahedral symmetry, the tensor reduces to a scalar quantity.

Defect symmetry is an important clue to the nature and structure of the defect. The measurement of the quantities necessary to determine the g-tensor was therefore our main concern. The determination of the g-tensor simply involved the simultaneous measurement of both resonance frequency and magnetic field of the resonance spectrum as a function of the orientation of the magnetic field with respect to the crystalline axes of the silicon sample. Magnetic field determinations were made by sweeping the field at a constant rate, while at the same time marking the value of the field by watching the transit of the proton nuclear magnetic resonance pattern of the gaussmeter on the oscilloscope screen. Markers were made on the recorder chart at intervals of approximately 10 oersteds by setting the gaussmeter oscillator at predetermined frequency intervals. The marker pen in the recorder was operated manually. Nuclear magnetic resonance frequencies could be determined with considerable accuracy; during the NMR scope pattern transit, the frequency did not change by more than one part in 10^5. In the magnetic field determination, frequency drifts can therefore be safely neglected. Major uncertainties in the magnetic field determination may therefore be attributed to the following sources: (a) uncertainties in locating the center of the proton "scope" pattern, (b) deviation of magnetic sweep from linearity, (c) uncertainty in locating the center of the resonance line from the nearest magnetic field marker, (d) demagnetization effects caused by paramagnetic impurities in the wall of the cavity (Reference 2), (e) difference in location between NMR probe and sample, (f) inhomogeneity over sample dimensions.

Calibration of the linear sweep with the NMR gaussmeter showed deviations from linearity to be about 140 millioersteds over a distance of 5 inches. Since the field markers were spaced about 2 inches on the recorder chart, one expects an uncertainty in the field determination of about 60 millioersteds. Uncertainties caused by (c) may be as much as 100 millioersteds. In order to find the effect of paramagnetic impurities in the brass cavity, calibration runs were made with the silicon g-marker obtained from E. A. Gere (Reference 21), and the magnetic field rotated through 120 degrees. Readings were taken of the magnetic field every 10 degrees with the NMR probe. These measurements showed the field as measured by the NMR probe to be consistently about 200 millioersteds higher than the field at the silicon g-marker (Figure 1), a value much too large to be accounted for by the difference in position of the NMR probe and the sample. This value also happens to be in good agreement with the value for the apparent g-shift for a brass cavity given by Feher (Reference 2), about 10^{-4}. The other uncertainties

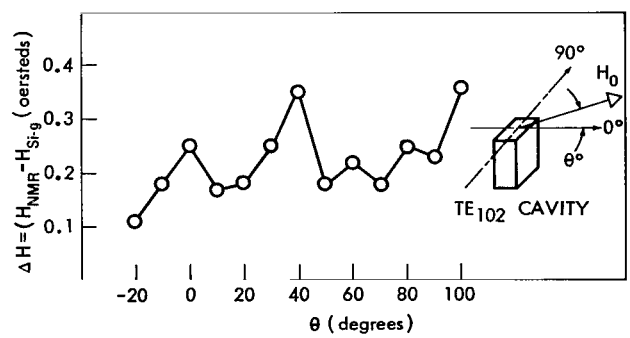

Figure 1—Demagnetization effect of the brass TE_{102} cavity; difference in magnetic field H_0 between nuclear magnetic resonance probe and silicon "g" marker as a function of the orientation of H_0.

(a), (e) have already been mentioned, and (f) is too small to contribute. From the random magnetic field uncertainties (a), (b), and (c), we find a probable error in H_0 of ±130 millioersteds, and from (d) and (e) a systematic error of +225 millioersteds. The random magnetic field error corresponds to a P.E. in the g-factor of ±0.0001, the systematic error to an error in "g" of 0.00014. The total error in the g-factor (systematic plus random) is then ±0.00025 uncorrected for demagnetization. When correction for demagnetization is made, we have to include the P.E. of the g-marker g-value, which is ±0.0001 (Reference 2), in our P.E. caused by the random magnetic field errors. So that the total P.E. in the g-value corrected for demagnetization becomes ±0.00015.

EXPERIMENTAL RESULTS

Lithium-Diffused Floating-Zone Silicon, (Li-O) Complex Resonance

All experiments on lithium diffused silicon were done with floating zone material in the 200 to 400 ohm-cm range. Most of the data were obtained for material grown by Wacker-Chemie GMBH.* Qualitative data were obtained for silicon grown by Texas Instruments Inc.† Table 1 gives a summary of the silicon specimens used and their resistivities after lithium diffusion. With the single exception of the Texas Instrument samples 1 and 1a whose 20 × 9 mm faces were oriented in the ⟨111⟩ direction, all samples were cut as described earlier.

Table 1

No.	Sample	Manufacturer	Dopant	Resistivity (ohm-cm)	Resistivity, lithium-diffused (ohm-cm)
1	SiPTiFZ200/3/31/66-3	Texas Instr.	Phosphorus	190	0.43 (Li-O)
1a	SiPTiFZ200/3/31/66-4	Texas Instr.	Phosphorus	190	0.1 only irrad.
2	SiPWaFZ300S94818-2	Wacker-Chemie	Phosphorus	240	1.0 (Li-O) and irrad.
3	SiPWaFZ400S5488A-2	Wacker-Chemie	Phosphorus	380	0.16 Li-donor
4	SiPWaFZ300S94818-1	Wacker-Chemie	Phosphorus	220	0.03

It is clear from the earlier discussion that one of the primary objectives in dealing with ESR of lithium donors and complexes must be the proper identification of the "lithium" resonance. Feher (Reference 2) made a determination of the g-tensor of the (Li-O) complex at K-band frequencies. He was able to describe the observed spectrum by an axially symmetric g-tensor with the axis of symmetry in the ⟨111⟩ direction, and an effective spin of 1/2. At K-band frequencies, the spectrum (consisting of four lines because of the four equivalent ⟨111⟩ directions of the defect with the magnetic field) is partially resolved; at X-band frequencies, not at all. Identification can be made at X-band by measuring the g-value of the resonance line with the magnetic field parallel

*Wacker-Chemie GMBH, Munich, West Germany; U.S.A. representative, Henley Co. Inc., 202 East 44th Street, New York, N. Y.
†Texas Instruments, Inc., Chemical Materials Dept., 13500 N. Central Expressway, P.O.B. 5012, Dallas 22, Texas.

to the ⟨100⟩ direction of the silicon crystal. It can easily be shown by considerations of the symmetry of the diamond lattice and the defect center that for this orientation only one microwave transition is observed. All possible four transitions fall on top of each other. Additional characteristics aiding in identification of the Li-O ESR transition are line width and dependence on external and internal stresses.* In our experiments, no predetermined stresses were introduced, but sample mountings in the cavity were varied to produce different stress situations. Feher (Reference 2) gives the components of the g-tensor as, $g_{\parallel}$ ⟨111⟩ = 1.9978 ± 0.0001 and $g_{\perp}$ = 1.9992 ± 0.0001; the g-factor is determined from

$$g^2 = g_{\parallel}^2 \cos^2 \alpha + g_{\perp}^2 \sin^2 \alpha , \qquad (1)$$

where α is the angle between the symmetry axis of the center and the magnetic field H_0. For H_0 parallel to the ⟨100⟩ direction, α is 54°44', giving a g-factor of 1.9987.

Resonances were observed in lithium-diffused, floating-zone phosphorus-doped silicon. Measurements were made with the field in the ⟨110⟩, ⟨111⟩, and ⟨100⟩ directions. The resonances had all the appearances of inhomogeneously broadened lines, with the lock-in detected output showing an absorption type envelope characteristic of many of the inhomogeneously broadened rapid passage cases discussed by Portis (Reference 12). All measurements were made in the dispersion mode and showed anisotropy with respect to the orientation of the magnetic field. No resolved structure could be observed; hence g-factor measurements were made with the field parallel to the ⟨100⟩ direction, with the assumption that we had found the resonance of the Li-O complex in floating zone material. The Li-O resonance was qualitatively identified in sample No. 1 of Table 1† and exhaustively studied in sample No. 2. Sample No. 4 could not be used because its resistivity proved too low for observation of resonance. Sample No. 3 gave a resonance which apparently was not caused by the Li-O complex and will be discussed at length later.

Measurements of the resonance were made with the sample mounted in the cavity in different ways in order to accentuate any stress effects. The different mounting procedures were discussed earlier; both Duco cement and styrofoam plugs were used. The average g-factor for H_0 parallel to the ⟨100⟩ direction turned out to be

$$g\left(H_0 \parallel \langle 100 \rangle\right) = 1.9985 \pm 0.00025 ,$$

with an average deviation from the mean for eight measurements of ±0.00012. No corrections were made for the apparent demagnetization effect of the cavity as discussed earlier. Line widths were measured at the half-power point (or at 0.7 of maximum resonance line intensity), and at half intensity. In all cases the total width of the resonance line was determined; i.e. $2\Delta H$, where ΔH is the half width. The results, again for the same eight runs were,

$$2\Delta H \text{ (half intensity)} = 2.7 \pm 0.1 \text{ oersteds}$$

*A great many other defects have g-values very close to (Li-O); therefore other corroborative information is desirable.
†Samples will henceforth be designated simply by numbers as shown in the first column of Table 1.

and,

$$2\Delta H \text{ (half power)} = 1.9 \pm 0.1 \text{ oersted}.$$

Feher (Reference 2) has shown that under fast passage conditions, one would expect the shape of the inhomogeneously broadened line to be the same whether the line is swept linearly or with magnetic field modulation. However, Feher observed that lines under field modulation were 5-10 percent broader and asymmetric. Since we were unable to record the lines using linear magnetic field sweep, we were unable to detect possible broadening of the lines. There appeared to be little asymmetry.

Feher's (Reference 2) value for the g-factor in the <100> direction is $g\left(H_0 \parallel \langle 100\rangle\right) = 1.9987$, and the line width of the resonance line in the <100> direction is $2\Delta H = 2.3 \pm 0.1$* oersted. It is not clear whether Feher's ΔH was measured at the half-power point or at half intensity. Our value of the g-factor is in very good agreement with Feher's value; however the discrepancy in line width, whether one considers the half power or half intensity is somewhat disturbing. It is possible that Feher's measurement refer to the width at the inflection point of the gaussian line shape or that our values are somehow affected by passage effects. The small deviation from the mean of our g-factor as well as the constant line width of the resonance gives us confidence that stress effects introduced by the various types of sample mountings play a minor role if any. We therefore conclude that the observed resonances in floating zone material are caused by (Li-O) complexes, and that Feher's lack of success in observing such resonances in his floating zone samples may be attributed to lower apparatus sensitivity. Figure 1 shows a typical record obtained for sample No. 2; it shows clearly aside from the resonance of the (Li-O) complex one line caused by the hyperfine interaction of the phosphorus donor electrons with the nuclear spin of the phosphorus nucleus. Since the phosphorus donor concentration is known from the room temperature resistivity of the floating-zone silicon before lithium diffusion, a comparison of the phosphorus donor resonance and (Li-O) resonance intensities may be a key to the oxygen concentration in floating-zone silicon.

Oxygen Concentration in Floating-Zone Silicon

Lithium donors are known to occupy interstitial positions in the silicon lattice (Reference 13) and consequently are highly mobile. It is therefore reasonable to assume that all available oxygen atoms in the lattice will be bound to lithium atoms into Li-O defects, which are detectable by spin resonance.† Comparisons of resonance intensities of inhomogeneously broadened lines under fast passage conditions can be very misleading unless one makes sure that both resonances were recorded under the same passage conditions. In order to determine which of the many rapid passage cases discussed by Portis (Reference 12) and Weger (Reference 14) is applicable, we have to find

*Resonance lines for Li-O seem to have been recorded with a linear sweep, and line width measurements were consequently unaffected by magnetic field modulation passage effects.

†This suggestion has also been made by B. Goldstein. See Reference 18.

out and, in some cases, assume what the experimental conditions were. We briefly list the experimental conditions of passage:

ω_m, modulation frequency:	400 Hz × 2π
dH_0/dt, linear field sweep:	1/12 oersted/sec
H_1, r.f. field in sample cavity, assuming Q_0 = 5000:	0.015 oersted
H_m, amplitude of magnetic field modulation:	~0.1 oersted
ΔH, line width:	approx. 2.5 oersted for both Li-O and phosphorus donor resonance
τ, relaxation time:	no determination of relaxation times was made, but τ is assumed to be on the order of tens of seconds for both species*

We find then, that with the above constants, the following general adiabaticity and saturation conditions are met:

(a) dH_0/dt and $\omega_m H_m < \gamma H_1^2$, $\gamma = 17.6 \times 10^6$ (oersted sec)$^{-1}$

and,

(b) $\gamma H_1 \tau > 1$.

In addition, the following special conditions are also met by both phosphorus and Li-O resonances:

(c) $\omega_m \tau > 1$, i.e. no relaxation during a modulation cycle

(d) $H_m > H_1$

(e) Conditions (c) and (d) imply that $H_m \omega_m \tau > 1 > H_1$, and we have rapid passage conditions through the individual spin packets.

(f) $\tau\, dH_0/dt < H_m$; i.e. the field interacts with a set of spin packets for a time at least equal to the relaxation time τ.

*According to G. Feher and E. A. Gere (Reference 21), the relaxation time in the concentration independent region for phosphorus donors at liquid helium temperature is about 25 seconds.

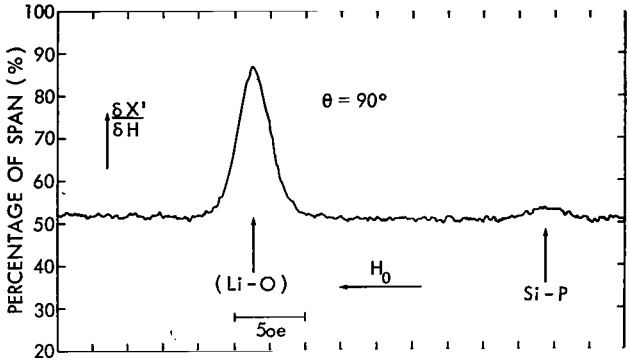

Figure 2—(Li-O) complex in floating-zone silicon, (240 ohm-cm), diffused with lithium to 1.0 ohm-cm, and low field resonance line of silicon-P HFS; $H_0 \parallel \langle 100 \rangle$. Sample No. 2. Gain 0.1, lock-in amplifier time constant 1.0 sec.

Portis calculates for these conditions a lock-in detector output signal which is 180 degrees out of phase with the modulation and a resonance line which has an absorption shape. It is possible that two of the above-mentioned conditions are only marginally met; this applies especially to (f), and perhaps to (d). The modulation amplitude was measured at room temperature; the amplitude would be considerably less at liquid helium temperature. However, experimental observation of the resonances (see Figure 2) gives us some confidence that the resonances correspond fairly close to passage case III-B given by Portis, with passage conditions as listed under (a) through (f). Both Li-O and phosphorus resonances show an absorption envelope with the lock-in component 180 degrees out of phase with the field modulation. No precise measurements were made of the phase angles, and there is a possibility that the observed resonances correspond to a mixture of the simplified cases discussed by Portis. Since both resonances have essentially the same line width and were recorded at approximately the same field, and we assume on the basis of the above passage case analysis approximately the same passage conditions for both "lines," the (Li-O) concentration can be scaled directly from Figure 2 and the known phosphorus concentration. According to an extrapolated plot of resistivity versus impurity concentration curves given by Irvin (Reference 15), we find a phosphorus concentration of 2×10^{13} cm^{-3}, and therefore a Li-O concentration of 10^{14} cm^{-3}. If our initial assumption concerning the lithium complexing behavior are correct, we have an oxygen concentration of 10^{14} cm^{-3} in the floating-zone material. This figure differs by about two orders of magnitude from the usually quoted values. One of the most recent determinations seems to be that of Hirata et al. (Reference 16), who quote a figure of 10^{16} cm^{-3} in floating-zone silicon with phosphorus concentrations from 10^{13}—10^{15} cm^{-3}. The determination is based on the 9-micron absorption band in silicon. It is difficult to believe that our estimate of the oxygen concentration is off by as much as a factor of 100 despite the uncertainties of the passage conditions. We may also mention Aggarwal et al. (Reference 4) measurements on lithium diffused floating zone silicon. They find that their measurements on floating zone silicon show no 9-micron band and conclude from this an upper limit to the oxygen concentration of about 10^{16} cm^{-3}.

Electron-Irradiated, Lithium-Diffused Silicon

Lithium-diffused silicon was irradiated with 1.0 Mev electrons to observe possible new defect centers and changes in intensity of (Li-O) complexes. Sample No. 2 (see Table 1) was irradiated with 1.0-Mev electrons with a total flux of 5×10^{15} electrons/cm^2. The irradiation time was 3 hours, and the sample temperature rise during this time not more than 1°C. Earlier, we presented fairly conclusive evidence that the originally observed center (i.e. before irradiation) was

the (Li-O) complex found and studied by Feher (Reference 2). Since this donor resonance has a singlet ground level (References 2 and 4), one would expect the irradiation to produce results which are not too different from those in phosphorus-doped silicon. See, for example Watkins, Corbett, and Walker (Reference 17). In other words, deep-lying energy levels associated with radiation-induced defects will accept electrons from the shallow donor levels,* and new resonances may be observed depending on the charge state of the radiation-induced defect. Figure 3 shows the sample resonance after irradiation. The conditions of observation are exactly the same as for the (Li-O) resonance shown in Figure 2. The magnetic field is in the <100> direction. Measurements of the irradiated sample were made with the H_0 field parallel to the <100>, <111>, and <110> directions. The resonance line in the <100> direction shows a definite but small increase in intensity of 10-15 percent and a decrease in line width of about 10 percent over resonances observed in the <111> direction. Intensity increase and sharpening of the line are somewhat less when compared with the resonance in the <110> direction. The g-factor was determined again for the <100> direction and found to be

$$g\left(H_0 \parallel \langle 100\rangle\right) = 1.9986 \pm 0.00025 ,$$

in excellent agreement with the g-factor found for the unirradiated sample. Considering then the anisotropy of the line as evidenced by changes in line width and intensity, as well as the excellent agreement of the g-factors in the <100> direction, we conclude that the observed line after irradiation is again the resonance of the Li-O complex but much reduced in intensity. Figure 4

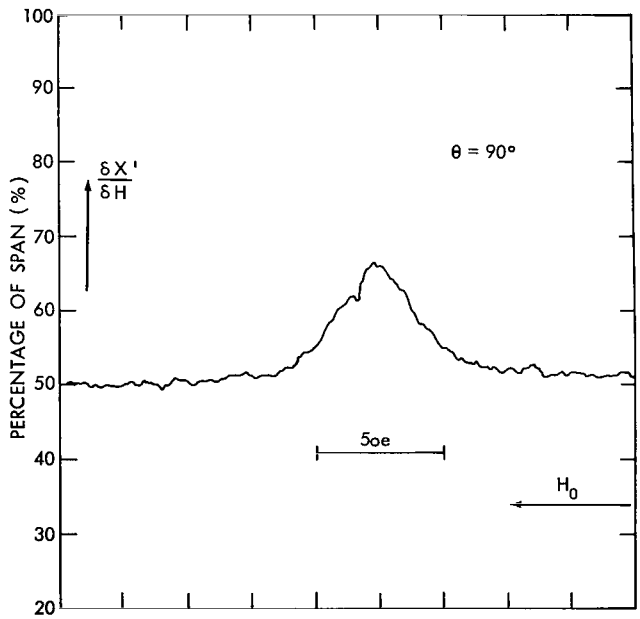

Figure 3—(Li-O) complex resonance in floating-zone silicon, (240 ohm-cm), diffused with lithium to 1.0 ohm-cm after irradiation with 5×10^{15} electron/cm^2 of 1.0 Mev. $H_0 \parallel \langle 100\rangle$. Gain 0.1, lock-in time constant 1.0 sec.

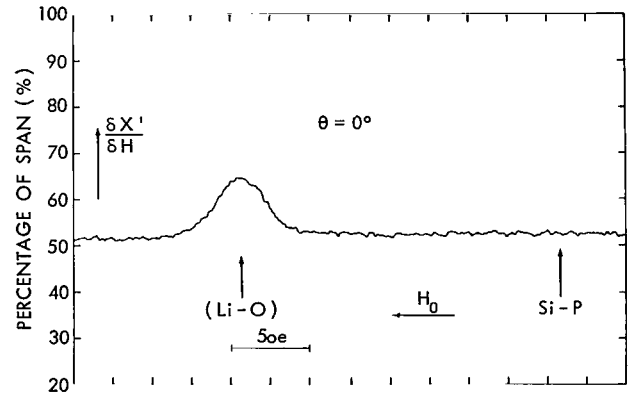

Figure 4—(Li-O) complex resonance of sample No. 2, floating-zone silicon after electron irradiation. $H_0 \parallel \langle 110\rangle$. Note absence of low field silicon-P HFS. Gain 0.1, time constant 1.0 sec.

*(Li-O) and Li donors have energy levels of about 0.039 and 0.033 ev, respectively, below the conduction band (see Reference 18).

shows, when compared with Figure 3, that the silicon donor resonance is gone; i.e. the silicon donor electrons have been trapped by deeper lying irradiation-induced defect levels.

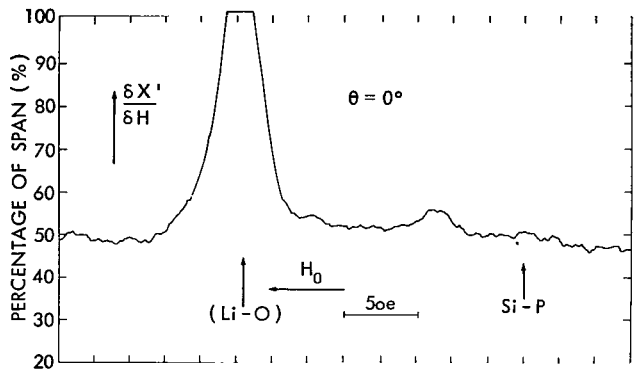

Figure 5—(Li-O) complex resonance of sample No. 2, floating-zone silicon, after electron irradiation. $H_0 \parallel \langle 110 \rangle$. Note resonance peak at g = 2.006, and absence of low field silicon-P HFS despite higher gain and longer time constant of lock-in. Gain 0.5, time constant 3 sec.

Similarly, the (Li-O) resonance shows a decrease of intensity of 54 percent. Hence the (Li-O) defects behave under electron irradiation like the shallow phosphorus donors. In order to see whether other paramagnetic defects were created by the radiation, the field was swept from g = 2.08 to g = 1.93 in the $\langle 100 \rangle$ direction with gain settings the same as in Figures 3 and 4. No resonances were observed. Figure 5 shows again the (Li-O) resonance after electron irradiation but recorded with higher gain settings,* with the magnetic field in the $\langle 110 \rangle$ direction. A small resonance peak can be seen on the low field side of the (Li-O) resonance. Runs were made in the $\langle 100 \rangle$, $\langle 110 \rangle$, and $\langle 111 \rangle$ direction. No exact "g" measurements were made because of the relatively low signal-to-noise ratio. But comparison of the records shows little if any anisotropy of the new resonance peak, which corresponds to a g-factor of 2.006. (We also notice that even at these higher gain settings, the phosphorus donor resonance is not visible.) The lack of any sort of structure, even the typical doublet of axially symmetric defects in the principal crystalline directions, makes any identification of the radiation-induced resonance with known defects such as C- and E-centers unlikely. Furthermore, the position of the Fermi level after irradiation of approximately -0.02 ev is another factor in the lack of E- or C-center resonances.

We briefly mention some qualitative results obtained with samples No. 1 and No. 1a. Earlier, the observed resonance in the unirradiated silicon sample No. 1 was qualitatively attributed to the (Li-O) complex. Subsequent irradiation of the sample at room-temperature with 1.0 Mev electrons and a total flux of 1×10^{17} electrons per cm^2 yielded again the (Li-O) attributed line, reduced in intensity by approximately a factor of ten. As in sample No. 2, the phosphorus donor resonances had disappeared. Subsequent runs of sample No. 1 yielded no significant changes in intensity of line shape, strong indication that we were looking at the Li-O complex.

Sample No. 1a with a lithium concentration of 8×10^{16} cm^{-3} was bombarded with a total dose of 1.0×10^{16} electrons per cm^2 with energy of 1.0 Mev. The resonance line after irradiation had the shape of the derivative of an absorption curve and did not reverse on magnetic field reversal, clearly an inhomogeneously broadened resonance signal as described by Portis' case IV. Subsequent ESR runs showed drastically changed signal shapes and amplitudes. Apparently this signal

*Gain settings for Figures 3 and 4 were 0.1, and a 1-second time constant for the lock-in amplifier; Figure 5 was recorded with a gain of 0.5, and a time constant of 3.0 seconds.

was similar to the ones reported by Goldstein (Reference 18) and at first tentatively attributed to a lithium vacancy complex. Later measurements by Goldstein (Reference 19) revealed the strain-dependence of the observed ESR lines after irradiation and lack of consistent results, with which, in this particular instance we agree.

Lithium-Diffused, Floating-Zone Silicon–Lithium Donor Resonance

The discussion of the lithium donor ground state earlier and the qualitative results mentioned in the last paragraph of the preceding section would seem to make this section superfluous. But we found that our results of what could only be the lithium donor resonance in sample No. 3 were fairly reproducible. Repeated ESR runs with the sample dismounted between runs gave reproducible line width, intensity, and g-factors. Further, the resonance line showed interesting properties: narrow line shape, anisotropy, structure, and slow passage characteristics.

The ESR spectra of sample No. 3 presented in this section are distinctly different from the spectra of the lithium-doped, floating-zone silicon of the preceding paragraphs. Figure 6 shows the resonance of the dispersion derivative for $H_0 \parallel \langle 100 \rangle$. The intensity compared to previously obtained resonances in lithium-diffused, floating-zone silicon was enormous, (note gain setting of lock-in amplifier of 0.001 compared to settings of 0.1 in Figure 7), which immediately led to the suspicion that we were looking at the Li donor electron resonance. The sample had been glued to the cavity walls with consequent stressing of the sample at the low temperature. A subsequent run with our "stress-free" cavity mount showed a resonance much reduced in intensity (about a factor of 100) still showing the characteristic derivative of dispersion shape (see Figures 7 and 8). As pointed out previously, reasonably consistent results could be obtained with this sample mounted with styrofoam. All subsequent discussion in this section concerns itself solely with the properties of the lithium ESR resonance obtained under stress-free conditions, except where noted. We briefly mention some data on the "stressed" sample of Figure 6. The resonance showed a line width (measured at half intensity of the dispersion derivative) of $2\Delta H = 0.56$ oe $\pm$ 0.05 with H_0 in the $\langle 100 \rangle$ direction,

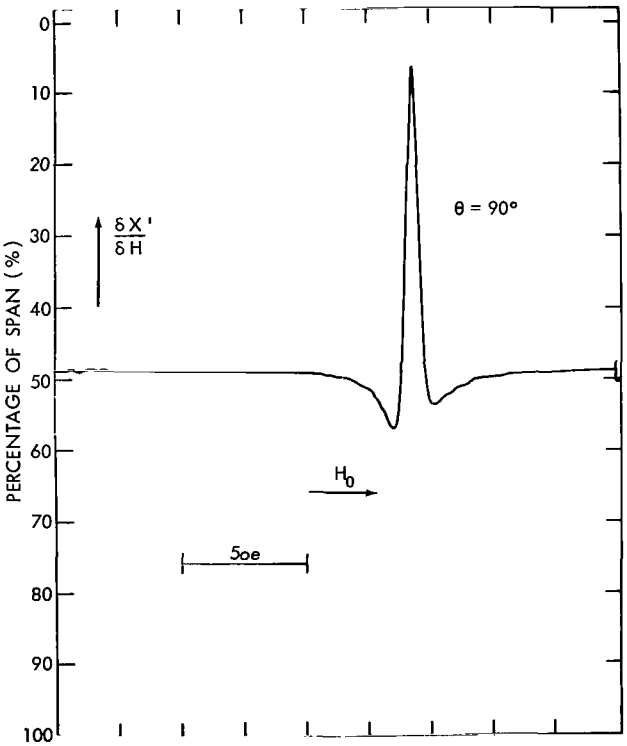

Figure 6—Lithium donor resonance in floating-zone silicon, (380 ohm-cm), diffused with lithium to 0.16 ohm-cm. Derivative of dispersion. Sample No. 3. $H_0 \parallel \langle 100 \rangle$. Gain 0.001, time constant 1.0 sec. Note absence of line splitting.

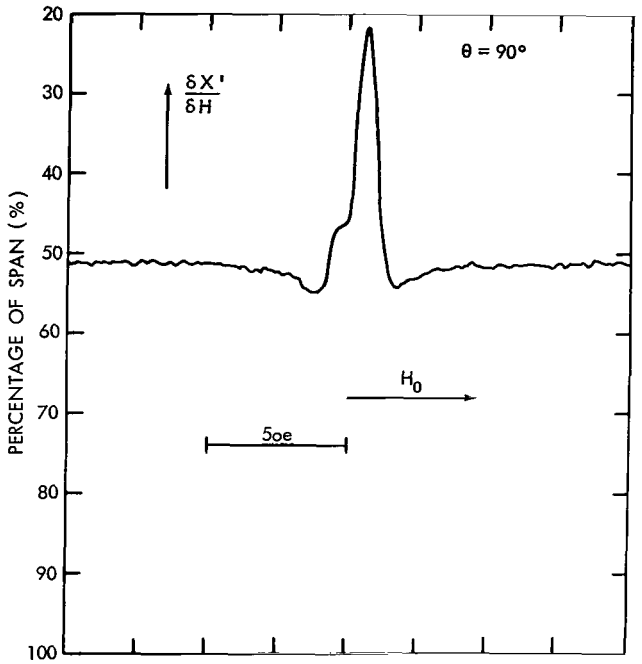

Figure 7—Lithium donor resonance in floating-zone silicon (380 ohm-cm) diffused with lithium to 0.16 ohm-cm. "Stress free" sample mount. Derivative of dispersion. $H_0 \parallel \langle 100 \rangle$. Sample No. 3. Gain 0.1, time constant 1.0 sec. Note splitting of resonance line.

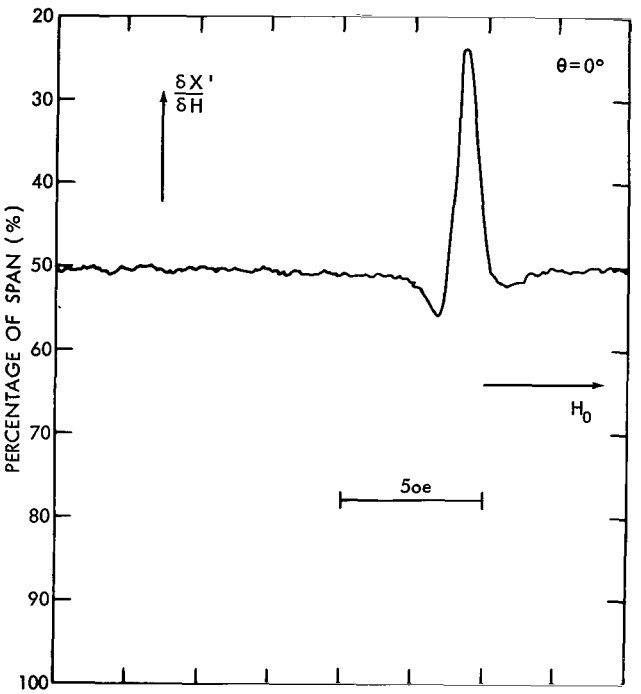

Figure 8—Lithium donor resonance in floating-zone silicon (380 ohm-cm) diffused with lithium to 0.16 ohm-cm. "Stress free" sample mount. Derivative of dispersion. $H_0 \parallel \langle 110 \rangle$. Sample No. 3. Gain 0.1, time constant 1.0 sec. Note splitting of resonance line.

and a slight anisotropy in the g-factor,

$$g\left(H_0 \parallel \langle 100 \rangle\right) = 1.99859 \pm 0.00025^{*\dagger} ,$$

$$g\left(H_0 \parallel \langle 111 \rangle\right) = 1.99895 \pm 0.00025 ,$$

$$g\left(H_0 \parallel \langle 110 \rangle\right) = 1.99906 \pm 0.00025 ,$$

which is, however, within the probable error of the measurements.

The "unstressed" sample showed some variation in line width and little change in intensity and g-factor after the sample had been brought back to room temperature and remounted in the cavity several times. Figures 7 and 8 show the dispersion derivative of the "unstressed" sample with a linewidth of $2\Delta H \approx 0.80$ oe $\pm$ 0.05, $H_0 \parallel \langle 100 \rangle$ and the following g-factors:

$$g\left(H_0 \parallel \langle 100 \rangle\right) = 1.99885 \pm 0.00025^{*\dagger} ,$$

*Uncorrected for demagnetization of cavity.
†Dispersion derivative.

$$g\left(H_0 \parallel \langle 111\rangle\right) = 1.99904 \pm 0.00025^{*\dagger},$$

$$g\left(H_0 \parallel \langle 110\rangle\right) = 1.99910 \pm 0.00025.$$

A different run of the same sample with the bridge tuned to absorption but all other conditions as in the preceding run gave the following results: $2\Delta H\left(H_0 \parallel \langle 100\rangle\right) = 0.90$ oe $\pm$ 0.05, (width measured between inflection points of absorption derivative) and,

$$g\left(H_0 \parallel \langle 100\rangle\right) = 1.99893 \pm 0.00025^{*\dagger},$$

$$g\left(H_0 \parallel \langle 111\rangle\right) = 1.99910 \pm 0.00025,$$

$$g\left(H_0 \parallel \langle 110\rangle\right) = 1.99906 \pm 0.00025;$$

g-values corrected for demagnetization are

$$g\left(H_0 \parallel \langle 100\rangle\right) = 1.99908 \pm 0.00015,$$

$$g\left(H_0 \parallel \langle 111\rangle\right) = 1.99928 \pm 0.00015,$$

$$g\left(H_0 \parallel \langle 110\rangle\right) = 1.99921 \pm 0.00015.$$

See Figures 9 and 10.

We note that the average deviation of the mean from the mean of $g\left(H_0 \parallel \langle 100\rangle\right)$ for the three sets of data is only 0.00013, whereas changes in line width are on the order of approximately 30 percent. Figures 7 through 10 show the emergence of some structure when $H_0 \parallel \langle 100\rangle$. It is to be noted that this structure was absent in the stressed sample whose ESR dispersion derivative is shown in Figure 6 with $H_0 \parallel \langle 100\rangle$ (nor was there any structure in the $\langle 111\rangle$ and $\langle 110\rangle$ directions).

In order to investigate the structure and nature of the lithium resonances in the unstressed sample in greater detail, the g-factor of the resonances of Figures 9 and 10 was

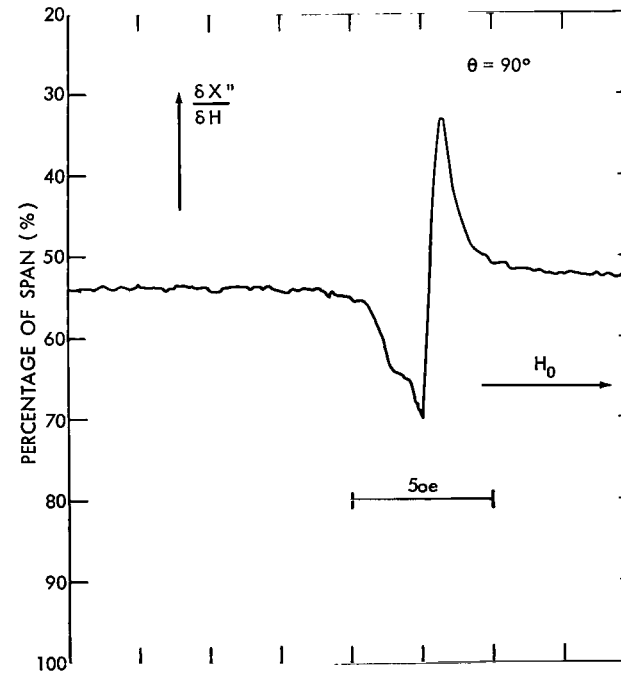

Figure 9—Lithium donor resonance in floating zone silicon, (380 ohm-cm), diffused with lithium to 0.16 ohm-cm. Sample No. 3. Derivative of absorption. "Stress free" sample mount. $H_0 \parallel \langle 100\rangle$. Gain 0.1, time constant 1.0 sec.

*Uncorrected for demagnetization of cavity.
†Absorption derivative.

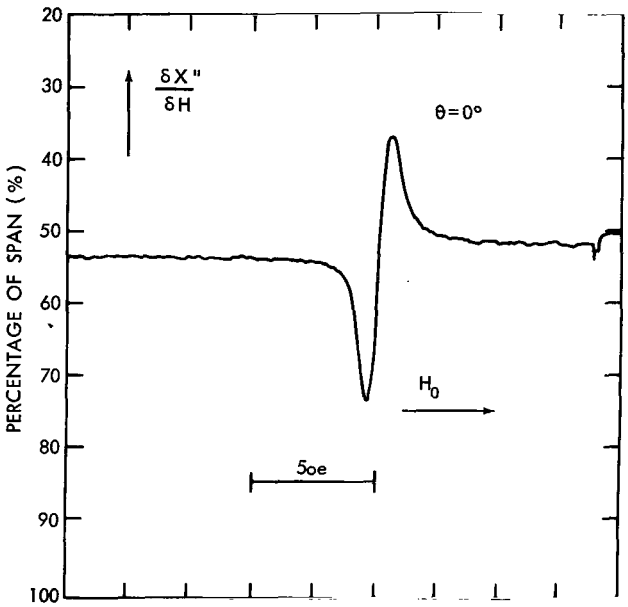

Figure 10—Lithium donor resonance in floating zone silicon, (380 ohm-cm), diffused with lithium to 0.16 ohm-cm. Sample No. 3. Derivative of absorption. "Stress free" sample mount. $H_0 \parallel \langle 100 \rangle$. Gain 0.1, time constant 1.0 sec.

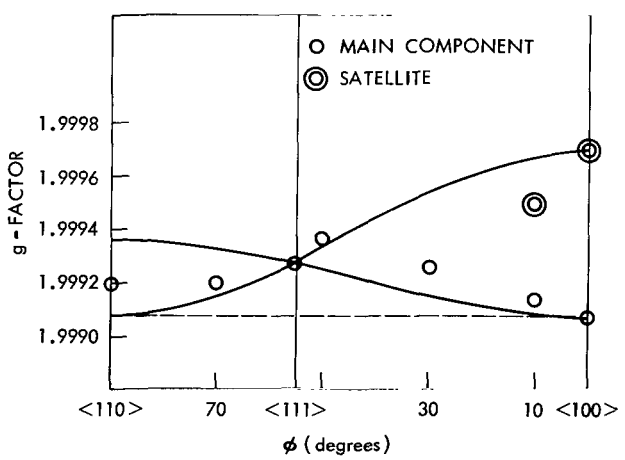

Figure 11—Angular dependence of the lithium donor resonance as a function of the orientation of the magnetic field H_0. Sample No. 3. "Stress free" sample mount. The data have been corrected for the demagnetization effect of the cavity. See Figure 1.

determined every 20 degrees from θ = -20 degrees to θ = 100 degrees, where θ is the angle of the magnetic field H_0 with the $\langle 110 \rangle$ direction in the $\{110\}$ plane. Similarly, saturation measurements were made with $H_0 \parallel \langle 110 \rangle$ over a power range of 27.8 db. The results of these measurements are shown in Figures 11 and 12. The variation of the lithium ESR spectrum with magnetic field orientation shown in Figure 11 gives the data corrected for the cavity demagnetization effect shown in Figure 1. The data were obtained by measuring the magnetic field at the crossover point of the absorption derivative. Doubtless, the asymmetries of the resonance line presumably caused by the superposition of two (or perhaps more) components, and not by a microwave bridge unbalance,* contribute to the g-value uncertainties.

Although we shall postpone a discussion of the doublet structure seen in Figures 7 and 9, we mention here that the structure emerges at θ = 80 degrees; it can be seen at 90 degrees and 100 degrees, but no structure is seen at 60 degrees.

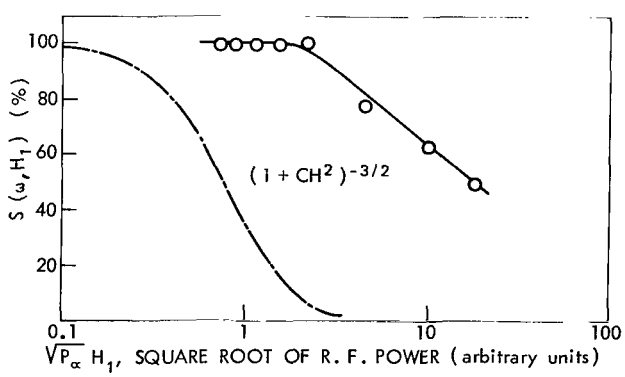

Figure 12—Saturation of absorption derivative of lithium donor resonance in floating-zone silicon, (380 ohm-cm), Sample No. 3. $H_0 \parallel \langle 100 \rangle$. The experimental curve is a plot of the observed values of the parameter $S(\omega, H_1) = \left[\delta\chi''/\delta\omega(H_1)\right]_{max} / \left[\delta\chi''/\delta\omega(H_1 = 0)\right]_{max}$ the dashed curve a plot of Equation 3.

*Klystron frequency locked to sample cavity.

The shift of the weaker satellite of the doublet with respect to the line of greater intensity is given by the changes of the g-factor relative to the latter:

$$\Delta g(\theta = 80°) = +0.00038 ,$$

$$\Delta g(\theta = 90°) = +0.00061 ,$$

$$\Delta g(\theta = 100°) = +0.00036 .$$

The g-factors of the satellite line are shown in Figure 11.

The appearance of the resonance line (see Figures 7 and 8) has all the earmarks of a line traversed under slow passage conditions and the narrow line width which Feher (Reference 2) observed for homogeneously broadened conduction electron resonances of heavily phosphorus-doped silicon. In order to find out more about the nature of the resonance, especially whether it is homogeneously or inhomogeneously broadened, measurements were made of saturation and line width as a function of saturation. All measurements were made on the derivative of the absorption with the klystron locked to the sample cavity.

Saturation measurements were made according to the progressive saturation method of Bloembergen, Purcell, and Pound (Reference 20). The power level on the sample* was progressively increased from 46 db† to 18 db† below klystron power (approx. 230 mw). Figure 12 shows the results of the measurements. The ordinate is a plot of the ratio

$$\left[\frac{\delta\chi''}{\delta\omega}(H_1)\right]_{max} \Big/ \left[\frac{\delta\chi''}{\delta\omega}(H_1 = 0)\right]_{max} = S(\omega, H_1) \qquad (2)$$

as a function of the square root of the r.f. power incident on the cavity in arbitrary units. As long as no saturation occurs, $S(\omega, H_1) = 100$ percent. Enough power was applied to achieve 50 percent saturation. Assuming a homogeneously broadened line with $\omega_m T_1 < 1$ (the relaxation parameter s follows the magnetic field modulation), Bloembergen, Purcell, and Pound (Reference 20) find

$$S(\omega, H_1) = (1 + s)^{-3/2} , \qquad (3)$$

where $s = \gamma^2 H_1^2 T_1 T_2$. A plot of the function $(1 + s)^{-3/2}$ is also shown for comparison. It is clear that the experimental results are very far indeed from the $(1 + s)^{-3/2}$ relation, nor do they fit a $(1 + s)^{-1/2}$ dependence. Saturation appears to take place much more slowly. We may conjecture here that the sample temperature may not be constant. The sample is submerged in liquid helium, but there seems to be the possibility that at high microwave powers the liquid helium gets partially boiled out of the cavity because of eddy current heating of the cavity walls and the sample itself.

*The cavity was near match.
†This includes the 3-db loss in the magic "T" of the bridge.

The relaxation rate in the region near 4.2°K is a sensitive function of temperature even in the concentration-dependent region.* It is interesting to note that a saturation curve drawn through all but the last two points corresponding to $P^{1/2} \propto 10$, and 18 (i.e., only to 78 percent saturation) has a slope which matches the theoretical curve quite closely.† Unfortunately there is no theoretical analysis of the saturation behavior of the derivative of the absorption for an inhomogeneously broadened line which could be used for comparison with the experimental data.‡

Line width measurements over the same range of r.f. power level variations as for the above saturation experiments showed a definite increase in line width of approximately 30 ± 8 percent§ (i.e., from 0.80 oe at 46 db to 1.1 oe at 18 db below klystron power). Line widths were measured between inflection points of the absorption derivative. The increase in line width of the absorption derivative (derivative of a Lorentzian line) of a homogeneously broadened line because of saturation is 40 percent when $\left(\delta\chi''/\delta H H_1\right)_{max}$ is a maximum. The condition for this maximum is $2T_1 T_2 \gamma^2 H_1^2 = 1$, which corresponds according to Equation 3 to $S(H_1, \omega) = 54.4$ percent (see J. S. Hyde, Reference 22). The absorption derivative did not show the expected maximum at $S(H_1, \omega) = 54.4$ percent, which we attribute to the increased temperature of the sample rather than inhomogeneous broadening.♦ Portis (Reference 12a) has shown that an inhomogeneously broadened absorption line does not change shape on saturation. The increase in line width is very strong evidence for a homogeneously broadened line.

Measurements were made on the derivative of absorption of the resonance of sample No. 3 to determine line shape. Inasmuch as the resonance line showed unresolved structure, this measurement seemed to be of doubtful value. A resonance was chosen, therefore, of reasonably symmetric shape. The results of these measurements showed that the line shape fell somewhere between a gaussian and a Lorentzian shape (Table 2).

Table 2

Shape of Gaussian, Lorentzian, and Observed Lines.*

Height (% of Ma.)	Gaussian	Position Lorentzian	Observed
100	a	a	a†
80	1.5a	1.65a	1.5a
60	1.8a	2.1a	1.8a
40	2.1a	2.75a	2.2a
20	2.5a	3.8a	3.3a
10	2.8a	5.0a	4.8a

*See Reference 31.

†"a" is the position of the maximum of the derivative of the absorption from the crossover point of the derivative.

*G. Feher and A. Gere (see Reference 21) give the temperature-dependence of the relaxation rate $1/T_s$ in the concentration-dependent region in Figure 6. The relaxation rate varies approximately as T^4 for phosphorus donors.

†i.e. $(1+s)^{-3/2}$.

‡Portis' analysis (Reference 23) of the saturation behavior of inhomogeneously broadened lines applies to power modulation detection schemes and not to magnetic field modulation signal detection.

§If we exclude data derived from the two high power measurements (i.e. points $P^{-1/2} \alpha 10$ and 18 in Figure 12) because of possible changes of temperature as discussed above, the line width increase corresponding to $P^{-1/2} \alpha 4.5$ is 15 percent.

♦A similar behavior was observed in the Si g-marker sample supplied by A. E. Gere. Feher reported the resonance lines of nonlocalized electrons to be homogeneously broadened. See Reference 2.

Lithium Donor Electron g-Tensor

The work of Aggarwal et al. (Reference 4) and Watkins (Reference 7) has clearly shown that the lithium donor electron in silicon is not in a singlet ground state. Electron spin resonance of lithium-diffused silicon should therefore show, aside from external and internal stress effects, a spheroidal g-tensor. The conduction electron g-tensor when averaged over the wave functions of a donor electron in the singlet state is isotropic and becomes $g = 1/3\ g_{\parallel} + 2/3\ g_{\perp}$ (Reference 24). If the group-V-like ground state is "inverted," the donor electron will be in a triplet state T_1. Electrons will also be in the doublet state E either degenerate with T_1 or separated from it by E_{23}, much smaller than the valley-orbit splitting E_{12} (Reference 10). Donor electrons in a triplet state will no longer have an isotropic g-tensor, but their electron spin resonance is presumably broadened beyond recognition because of the triplet (and doublet) degeneracy and consequently is unobservable (Reference 7). Calculations have been made by Roth and Lax (Reference 25) on the g-tensor of a donor electron in a triplet state in germanium. They find that for H_0 in an arbitrary position in a $\langle 110 \rangle$ plane, three resonances should be observed. Anisotropy has been observed in the g-tensor of antimony-donor electron resonances (References 26, 27, and 28) in germanium which is attributed to the small value of the valley-orbit (singlet-triplet) splitting (0.399×10^{-3} ev, Reference 28) and consequent admixture of the triplet state into the singlet by local strains. The admixture of the triplet state may also be interpreted as a change in the valley population. Thus Keyes and Price (Reference 29) have accounted for the "new" four-line spectrum observed by Pontinen and Sanders (References 27 and 28) in antimony-doped germanium by assuming high local strains in the crystal—high enough to cause the electrons to occupy a single valley. Electrons populating this valley would have a g-tensor $g^2 = g_{\parallel}^2 \cos^2\phi + g_{\perp}^2 \sin^2\phi$ (Reference 25), where ϕ is the angle of the symmetry axis of the valley with the magnetic field and $g_{\parallel}$ and $g_{\perp}$ are the principal g-values. The four-line spectrum can be attributed to donor electrons in the four conduction band valleys with spheroidal g-tensors. The valleys are selectively occupied in different regions of the crystal depending on the local strain situation.

The resonance spectrum of sample No. 3 shown in Figures 7 through 10 shows an almost resolved structure in the $\langle 100 \rangle$ direction and anisotropy. Previous results on silicon-Li have shown either narrow isotropic lines (Reference 1), resonances attributed to the (Li-O) complex (Reference 2), or an anisotropic stress-sensitive spectrum whose line width, intensity, and g-factor depended on externally applied uniaxial stresses (Reference 7). The latter observed by Watkins is especially interesting because it was the first evidence obtained by ESR that the lithium donor electron ground state is not a singlet. No data were given on the anisotropy of the spectrum. The stress-sensitivity of our sample leaves very little doubt that the observed resonances were caused by donor electrons in the triplet state (see Figure 6). The stress-free resonances shown in Figures 7 through 10 are very likely caused by lithium donor electrons also in the triplet (and doublet) state whose degeneracy has been lifted by local internal strains.* Although one expects an anisotropic g-tensor for donor electrons in a triplet ground state, a resolved anisotropic spectrum has to our knowledge never been reported. Both our "stressed" sample (Figure 6) and our "unstressed"

*The resonance shown in Figure 6 had obviously been affected by the external strains introduced by the particular mounting of the sample in the cavity.

sample (Figures 7-10) showed some anisotropy even when corrections for demagnetization of the cavity were made (see Figure 11). We will make the assumption that the observed resonance lines of the "unstressed" sample can be explained by using the suggestions by Keyes and Price (Reference 29); i.e., highly localized internal strains cause the lithium donor electrons in silicon to occupy a single valley in a particular region of the crystal. For donor electrons in a single valley, we have $g^2 = g_{\parallel}^2 \cos^2\phi + g_{\perp}^2 \sin^2\phi$, where the symbols are as explained above and ϕ is now the angle of the magnetic field H_0 with the $\langle 100 \rangle$ principal valley axis. In all our experiments H_0 was confined to rotate in a $\{110\}$ plane. For an arbitrary direction of H_0, six resonances will appear, but with H_0 in a $\{110\}$ plane, half of the six $\langle 100 \rangle$ valley symmetry axes will make the same angle with H_0, reducing the maximum number of observable resonances to three. The spectrum reduces to two lines ($\phi = 0°, 90°$) when H_0 is in the $\langle 100 \rangle$ direction and similarly when H_0 is parallel to $\langle 110 \rangle$, and $\phi = 90°$ and 45°. However, with H_0 in a $\langle 111 \rangle$ direction, the valley symmetry axes make an angle of 54°44' and 125°15' giving the same g-value. From these considerations, one expects the splitting of the resonance lines to be largest in the $\langle 100 \rangle$ direction and to be equal to $|g_{\parallel} - g_{\perp}|$, the line width narrowest, and the line intensity to be largest in the $\langle 111 \rangle$ direction. Since the line structure is barely resolved in the $\langle 100 \rangle$ direction, the observed resonance in the $\langle 110 \rangle$ direction will be unresolved and broad. The experimental observations tend to confirm this. See Figures 7 and 8. The resonance in the $\langle 111 \rangle$ direction is narrower and more intense than either the $\langle 100 \rangle$ or $\langle 110 \rangle$ transitions; line width (full width at half height) is 0.76 oersted, and intensity is 40 units. The g-tensor with $\langle 100 \rangle$ axial symmetry also allows us to determine the principal g-values, since the doublet resonance in the $\langle 100 \rangle$ direction corresponds to the two g-value $g_{\parallel}$ and $g_{\perp}$ (Reference 30). However, assignment of which of the two values is larger depends on a theoretical knowledge of the relative intensities of the lines. We find for the two g-values (corresponding to the principal values of g), in the $\langle 100 \rangle$ direction $g = 1.99969 \pm 0.00015$, and 1.99908 ± 0.00015. If we assume $g_{\parallel} > g_{\perp}$ and calculate $g\left(H_0 \parallel \langle 111 \rangle\right)$, using the above experimental values, we get $g\left(H_0 \parallel \langle 111 \rangle\right) = 1.99927$, in excellent but no doubt fortuitous agreement with the observed value of 1.99927. Similarly we find for the g-factor in the $\langle 110 \rangle$ direction, 1.99939 and 1.99908. This doublet was unresolved with an observed g-factor of 1.99921 and is in fair agreement with the calculated values. We conclude, therefore, with a fair degree of certainty that the anisotropic resonance spectrum observed in the lithium-diffused silicon sample No. 3, (0.16 ohm-cm) has a spheroidal g-tensor with $\langle 100 \rangle$ axial symmetry. Highly localized strains in the crystal not only lift the degeneracy of the triplet ground state but are such that the donor electron wave function arises from single valleys and different valleys in different parts of the crystal. We may also note that Wilson and Feher (Reference 10) found in their stress experiments on phosphorus-doped silicon $\left(g_{\parallel} - g_{\perp}\right) = +1.04 \times 10^{-3}$ compared to our value of $+0.68 \times 10^{-3}$ for lithium donors. Although the probable error in our "g" measurements after correction for demagnetization is ±0.00015, the partially resolved structure makes the error in $g_{\parallel} - g_{\perp}$ and $g_{\parallel}$ much larger and difficult to determine.

ACKNOWLEDGMENTS

I would like to express my gratitude to Mr. M. Schach for his unfailing and generous support of this work. It is a great and special pleasure to acknowledge Prof. R. H. Sands' invaluable

suggestions and great patience in explaining to me microwave bridge operation, and his generous loan of a L4154 diode. I am extremely grateful to Prof. A. M. Portis for explaining to me some fine points of his fast passage effects, and to Dr. G. D. Watkins for discussing with me at some length many aspects of ESR in silicon. I am indebted to Dr. P. Fang for suggesting the problem, and Dr. F. Patten, Dr. D. P. Snowden, and Dr. E. G. Wikner for helpful discussions. Many thanks are due Mr. W. Wappaus for his patient efforts to produce reproducible and clean lithium diffusions. I would like to express my appreciation for a lithium-diffused silicon sample made available to us through the kindness of Dr. J. J. Wysocki, and for Mr. A. E. Gere's extremely helpful g-marker sample. Many thanks are also due Mr. S. Brashears for his help in all phases of ESR measurements and data reduction, and to Mrs. R. Tauke for allowing me to copy her high sensitivity four point probe resistivity set up.

Goddard Space Flight Center
National Aeronautics and Space Administration
Greenbelt, Maryland, May 7, 1968
125-21-02-05-51

REFERENCES

1. Honig, A., and Kip, A. F., "Electron spin resonance of an impurity level in silicon," *Phys. Rev., 95,* 1686, 1954.

2. Feher, G., "Electron spin resonance experiments on donors in silicon; I: Electronic structure of donors by the electron nuclear double resonance technique," *Phys. Rev., 114,* 1219, 1959.

3. Feher, G., "Observation of nuclear magnetic resonance via the electron spin resonance line," *Phys. Rev., 103,* 834, 1956.

4. Aggarwal, R. L., Fisher, P., Mourzine, V., and Ramdas, A. K., "Excitation spectra of lithium donors in silicon and germanium," *Phys. Rev., 138,* A882, 1965.

5. Kohn, W., and Luttinger, J. M., "Theory of donor states in silicon," *Phys. Rev., 98,* 915, 1955.

6. Kohn, W., "Shallow Impurity States in Silicon and Germanium," *in Solid States Physics, 5,* page 257, Ed. F. Seitz and D. Turnbull, New York: Academic Press, 1957.

7. Watkins, G. D., "Electron spin resonance of isolated lithium donors in silicon," *Bull. Am. Phys. Soc., 10,* 303, 1965.

8. Hancock, R. D., and Edelman, S., "Simplified light reflection technique for orientation of germanium and silicon crystals," *Rev. Sci. Instr., 27,* 1082, 1956.

9. Geiger, F. E., and Brashears, S., "Optical alignment of silicon crystals," NASA Technical Note D-4187, Nov. 1967.

10. Wilson, D. K., and Feher, G., "Electron spin resonance experiments on donors in silicon; III: Investigation of excited states by the application of uniaxial stress and their importance in relaxation processes," *Phys. Rev., 124,* 1068, 1961.

11. Ludwig, G. W., and Woodbury, H. H., "Electron Spin Resonance in Semiconductors," in Solid State Physics Vol. 13, p. 223, Ed. F. Seitz and D. Turnbull, New York: Academic Press, 1962.

12. Portis, A. M., "Magnetic resonance in systems with spectral distributions," Tech. Note No. 1, Sarah Mellon Scaife Radiation Laboratory, University of Pittsburgh, Pittsburgh, Pennsylvania, November 15, 1955.

13. Weiser, K., "Theory of diffusion and equilibrium position of interstitial impurities in the diamond lattice," *Phys. Rev., 126,* 1427, 1962.

14. Weger, M., "Passage effects in paramagnetic resonance experiments," *Bell. Syst. Tech. J., 39,* 1013, 1960.

15. Irvin, J. C., "Resistivity of bulk silicon and of diffused layers in silicon," *Bell Syst. Tech. J., 41,* 387, 1962.

16. Hirata, M., Saito, H., and Crawford, J., "Recombination centers in gamma-irradiated silicon," *J. Appl. Phys., 38,* 2433, 1967.

17. Watkins, G. D., Corbett, J. W., and Walker, R. M., "Spin resonance in electron irradiated silicon," *J. Appl. Phys., 30,* 1198, 1959.

18. Goldstein, B., "Direct observation of lithium-defect interaction in silicon by electron paramagnetic resonance measurements," *Phys. Rev. Letters, 17,* 428, 1966.

19. Goldstein, B., Semiannual Progress Report No. 1, 21 June-20 November, 1966, David Sarnoff Research Center, Radio Corp. of America, Princeton, N. J.

20. Bloembergen, N., Purcell, E. M., and Pound, R. V., "Relaxation effects in nuclear magnetic resonance absorption," *Phys. Rev., 73,* 679, 1948.

21. Feher, G., and Gere, A., "Electron spin resonance experiments on donors in silicon; II: Electron spin relaxation effects," *Phys. Rev., 114,* 1245, 1959.

22. Hyde, J. S., "Experimental Techniques in EPR," Varian Associates, Analytical Instrument Div., Palo Alto, California, Nov. 11, 1963.

23. Portis, A. M., "Electronic structure of F-centers: saturation of electron spin resonance," *Phys. Rev., 91,* 1071, 1953.

24. Roth, L. M., "g factor and donor spin-lattice relaxation for electrons in germanium and silicon," *Phys. Rev., 118,* 1534, 1960.

25. Roth, L. M., and Lax, B., "g factor of electrons in germanium," *Phys. Rev. Letters, 3,* 217, 1959.

26. Feher, G., Wilson, D. K., and Gere, E. A., "Electron spin resonance experiments on shallow donors in germanium," *Phys. Rev. Letters, 3,* 25, 1959.

27. Pontinen, R. E., and Sanders, T. M., "New electron spin resonance spectrum in antimony-doped germanium," *Phys. Rev. Letters, 5,* 311, 1960.

28. Pontinen, R. E., and Sanders, T. M., "Electron spin resonance experiments on antimony-doped germanium," *Phys. Rev., 152,* 850, 1966.

29. Keyes, R. W., and Price, P. J., "Additional spin resonance spectrum in antimony-doped germanium," *Phys. Rev. Letters, 5,* 473, 1960.

30. Corbett, J. W., "Electron Radiation Damage in Semiconductors and Metals," in Solid State Physics, Ed. F. Seitz and D. Turnbull, New York: Academic Press, 1966 (see p. 51, Figure 22(b)).

31. "EPR Operating Techniques" in Instruction Manual, V-4502 EPR Spectrometer Systems, Varian Associates, Instrument Division Publication 87-100-123, Sections 5.9, 5.10, 5.11.

NASA-Langley, 1968 —— 26

"The aeronautical and space activities of the United States shall be conducted so as to contribute . . . to the expansion of human knowledge of phenomena in the atmosphere and space. The Administration shall provide for the widest practicable and appropriate dissemination of information concerning its activities and the results thereof."

—NATIONAL AERONAUTICS AND SPACE ACT OF 1958

NASA SCIENTIFIC AND TECHNICAL PUBLICATIONS

TECHNICAL REPORTS: Scientific and technical information considered important, complete, and a lasting contribution to existing knowledge.

TECHNICAL NOTES: Information less broad in scope but nevertheless of importance as a contribution to existing knowledge.

TECHNICAL MEMORANDUMS: Information receiving limited distribution because of preliminary data, security classification, or other reasons.

CONTRACTOR REPORTS: Scientific and technical information generated under a NASA contract or grant and considered an important contribution to existing knowledge.

TECHNICAL TRANSLATIONS: Information published in a foreign language considered to merit NASA distribution in English.

SPECIAL PUBLICATIONS: Information derived from or of value to NASA activities. Publications include conference proceedings, monographs, data compilations, handbooks, sourcebooks, and special bibliographies.

TECHNOLOGY UTILIZATION PUBLICATIONS: Information on technology used by NASA that may be of particular interest in commercial and other non-aerospace applications. Publications include Tech Briefs, Technology Utilization Reports and Notes, and Technology Surveys.

Details on the availability of these publications may be obtained from:

SCIENTIFIC AND TECHNICAL INFORMATION DIVISION

NATIONAL AERONAUTICS AND SPACE ADMINISTRATION

Washington, D.C. 20546